



Polyethylene glycol grafted chitin nanocrystals enhanced, stretchable, freezing-tolerant ionic conductive organohydrogel for strain sensors

Jiabing Cai, Yunqing He, Youquan Zhou, Hongbo Yu, Binghong Luo, Mingxian Liu^{*}

Department of Materials Science and Engineering, College of Chemistry and Materials Science, Jinan University, Guangzhou 510632, China

ARTICLE INFO

Keywords:

Polymer-matrix composites (PMCs)
Electrical properties
Electron microscopy
Surface treatments

ABSTRACT

Ionic conductive hydrogels with advantageous mechanical properties and high stretchability attract much attentions in wearable electronic devices. Here, a freezing-tolerant hydrogel with high stretchability (435%), strength (2.0 MPa), and ionic conductivity had been prepared by freezing/thawing of polyvinyl alcohol (PVA) and polyethylene glycol functionalized chitin nanocrystals (PEG-g-ChNCs) in dimethyl sulfoxide-water solvent. The successful grafting of PEG on ChNCs was confirmed by various characterization methods. The organohydrogel reinforced by PEG-g-ChNCs displayed excellent freezing-tolerance without rupture during extension, which remains conductivity (0.01 S/m) even at $-20\text{ }^{\circ}\text{C}$. PVA/PEG-g-ChNCs organohydrogel was employed as strain sensor. Interestingly, the sensors based on this organohydrogel presented high stretching sensitivity with a gauge factor of 2.3, and it could be repeatedly and stably monitor tiny strain under extension and pressure. Therefore, the ionic conductive organohydrogel sensor based PEG-g-ChNCs enhanced PVA have promising applications in wearable devices, such as sports monitoring or healthcare monitoring.

1. Introduction

In recent years, with the rise and development of internet of things and sensor technology, conductive hydrogel with high conductivity and mechanical properties (stretchable, flexible, compressible) has attracted numerous attentions in the field of wearable electronic devices, human-machine interaction [1–4], electronic skin and so on [5–7]. These conductive hydrogel sensors can transform external stimuli (temperature, pH, mechanical strain, magnet, etc.) into detectable electrical signals with high precision and sensitivity [8]. In practical applications, PVA hydrogels have good processability and biocompatibility, which are widely used in wearable devices and other biological materials [9,10]. Nevertheless, PVA hydrogels are often not strong enough which limits its large-scale use. At present, several solutions have been proposed, such as adding nano-materials [11,12], increasing the cross-linking density, and so on [13,14]. The introduction of nano-materials can effectively improve the mechanical performances. However, it is difficult for these nano-materials to be evenly dispersed in the PVA matrix, and the nanoparticles could disrupt the cross-linked PVA network structure [15,16]. Alternatively, tight cross-linked networks can increase mechanical performances, however, this can hinder ion mobility and conductivity. So, it is of practical significance to explore

conductive hydrogels with excellent mechanical strength, flexibility and conductivity.

Generally, conductive hydrogels are based on conductive polymer hydrogels, addition of conductive fillers, and ionic conductive hydrogels [17–20]. However, conductive polymers suffer from the high cost and limited types, and conductive fillers may be unevenly distributed to form aggregates. In contrast, ionic hydrogels can achieve high ionic mobility with free-moving ions [21]. Meanwhile, the conductivity of ionic conductive hydrogels is highly dependent on network structure and external stimuli.

Chitin is one of the most abundant polysaccharide in nature, second only to cellulose. It can be easily extracted from shellfish, fungi and insects. Chitin nanocrystals (ChNCs) obtained by removing amorphous domain of chitin are natural nanomaterials with needle shape, which display a several advantages including high aspect ratio, high specific surface area, high longitudinal modulus, and a large number of surface functional groups [22–25]. Unfortunately, when ChNCs are added directly to the polymer matrix, the high specific surface area of these nanoparticles will cause them to attract each other and form aggregates in several microns, which often greatly reduce the enhancement effect [26,27]. In order to solve this problem, Araki et al. prepared sterically stabilized ChNCs by grafting mPEG2000 via reductive amination

^{*} Corresponding author.

E-mail address: liumx@jnu.edu.cn (M. Liu).

between the surface amino groups on ChNCs and terminal aldehydes on mPEG2000, which improved in the dispersion stabilities of ChNCs and could potentially contribute to applications as reinforcing fillers [28]. Ifuku et al. grafted polyacrylic acid onto chitin nanofiber using potassium persulfate as a free radical initiator in an aqueous medium [29]. In our previous work, poly (L-lactide) (PLLA) was grafted onto the surface of ChNCs for improving the mechanical properties and biocompatibility of the PLLA matrix [30].

Conventional hydrogels usually freeze at temperatures below zero and become hard, brittle, and non-conductive, which limit its application at low temperature. Even at room or higher temperature, the moisture of hydrogels will evaporate quickly. Numerous work have been explored in order to improve the anti-freezing and moist properties of hydrogels. For example, some researchers used ethylene glycol or glycerol/H₂O binary solvent system to prepare freezing-tolerant organohydrogels [21,31,32]. Furthermore, anti-freezing PVA hydrogels were prepared by using mixing solvent of dimethyl sulfoxide (DMSO) and water, which can maintain thawing and mechanical flexibility even at -70°C . DMSO is a common anti-freezing agent as it can form strong hydrogen bonds with water molecules, which can destroy ice lattice and prevent water evaporation at temperature below zero. In addition, DMSO and water mixture in different proportions can adjust the freezing point flexibly. For example, when the molar ratio of DMSO to water is 7:3, the freezing point of water can reach -115°C [11]. More importantly, DMSO can also promote the gelation of PVA and significantly shorten the cycle time of freeze-thawing during gel preparation. As a result, DMSO has been used to make anti-freezing PVA organohydrogels in recent years [33],[34].

In this study, ChNCs were firstly modified with amino terminated polyethylene glycol (PEG) using polydopamine (PDA) as a linker. Then, an ionic conductive PVA organohydrogel was prepared in DMSO/water mixture solvent as well as a combination of PEG-g-ChNCs and immersion salt solution. The organohydrogel showed good mechanical properties, stability, and freezing-tolerant by good interfacial interactions between PEG-g-ChNCs and PVA matrix. DMSO as an anti-freezing agent has a higher dielectric constant, which helps ionic dissociation and improves conductivity. The organohydrogel was then employed as a strain sensor, which can detect human movement with high sensitivity, stability, and durability. All these results suggested that PVA organohydrogel sensor reinforced by PEG-g-ChNCs have great potential application in bionic skin, health monitoring and human-machine interactions.

2. Experimental section

2.1. Materials

Crab shells were supplied by Wuhan Hezhong Biochemical Manufacturing Co., Ltd., China. Hydrochloric acid (HCl, 37%) was obtained from Guangzhou Chemical Reagent Factory (Guangzhou, China). Tris-HCl buffer solution was bought from Sorebo Biotechnology Co., Ltd., China. Hydroxyphenethylamine hydrochloride (dopamine, 98%), amino-terminated PEG (the weight average molecular weight (Mw) was 1.0 kg/mol) and PVA (degree of alcoholysis was 99%, degree of polymerization was 1700), were purchased from Aladdin Reagent (Shanghai, China). DMSO was provided by Tianjin Fuyu Fine Chemical Reagent Factory (Tianjin, China). Deionized water was made in the laboratory. All the chemicals were directly used as received.

2.2. Surface functionalization of ChNCs

ChNCs powder was prepared by acid hydrolysis according to the previous study [35]. 20 g clean crab shells were hydrolyzed using 500 mL 3 mol/L HCl solution at 104°C for 3 h with mechanical stirring. Then, the mixture was washed by deionized water and centrifuged at 6000 rpm for 5 min for three times to remove by-product and excess

acid. The suspension was dialyzed in deionized water until it reached neutral. Finally, the suspension was lyophilized for 24 h in the vacuum freeze-dryer (Ningbo Scientz Biotechnology Co., Ltd., China) to obtain ChNCs powder.

PEG was grafted on ChNCs for surface functionalization according to the literature with slight modification [36]. The typical procedure was as below. 0.4 g ChNCs powder was immersed in 400 mL of buffer solution with ultrasonic treatment for 30 min and then 200 mg dopamine was added. The pH of the mixed solution was adjusted to 8.5 under magnetic stirring at room temperature for 12 h. The resulting mixture was centrifuged with deionized water for 3 times to remove free PDA. The solution was freeze-dried at -55°C for 24 h to gain PDA coated ChNCs (PDA@ChNCs). To acquire PEGylated ChNCs (PEG-g-ChNCs), the PDA@ChNCs was further dispersed into 300 mL of buffer solution (pH = 8.5) with ultrasonic treatment for 30 min. Then, 600 mg of amino-terminated PEG was added to the solution under magnetic stirring at 50°C for 24 h. Subsequently, the mixture was washed with deionized water by centrifugation to obtain black suspended solids, followed by freeze-drying for further use.

2.3. Fabrication of PVA/PEG-g-ChNCs organohydrogels

PEG-g-ChNC suspension was prepared by using ultrasonic treatment method. PEG-g-ChNC suspension (8 g, ≈ 0.444 mol H₂O) with different concentrations was added into DMSO (12 g) and stirred for 2 h to ensure PEG-g-ChNCs well dispersion. After that, PVA (1.8 g) was added to the suspension and heated to 90°C with adequate stirring until all PVA was fully dissolved. The PVA and PEG-g-ChNCs mixture was settled in the heating stage without stirring to remove air bubbles, and then it was transferred to a teflon mold and placed at -20°C for 24 h for gelation. By different concentration of PEG-g-ChNCs suspension, three different PVA/xPEG-g-ChNCs organohydrogels were fabricated (x refers to the weight ratios of PEG-g-ChNCs to PVA: 1%, 3%). The PVA/PEG-g-ChNCs organohydrogel was soaked in NaCl solution (0.05 M, 0.5 M, 1 M and 2 M, dissolved in DMSO/H₂O with the same weight ratio of 3:2) for 24 h to obtain ionic conductive organohydrogels.

2.4. Characterization

The morphology of ChNCs, PDA@ChNCs, and PEG-g-ChNCs were analyzed by transmission electron microscopy (TEM; JEM-1400Flash, JEOL, Japan). The particle size distribution and ζ potential of the ChNCs, PDA@ChNCs, and PEG-g-ChNCs aqueous dispersion were obtained using a nano ZS ζ -potential analyzer (Malvern Instruments Co., U. K.). Fourier transform infrared spectroscopy (FTIR) of ChNCs, PDA@ChNCs, PEG-g-ChNCs, PVA, and PVA/PEG-g-ChNCs was obtained with thermo FTIR (Nicolet iS50, Thermo Fisher Scientific Co. Ltd., USA). X-ray diffraction (XRD) patterns were recorded using a miniflex600 (Rigaku Corp, Japan) by Cu-K α radiation from 5° to 65° . The cross-section of PVA and PVA/PEG-g-ChNCs organohydrogels were prepared by brittle fracture of the sample in liquid nitrogen and then observed using a scanning electron microscope (SEM, Quanta400FEG, FEI, USA). XPS experiments of ChNCs and PEG-g-ChNCs powder were carried out on an ESCALAB250Xi (Thermo Fisher Scientific Ltd., USA). UV-vis spectroscopy (Lambda 35, PerkinElmer) were utilized to measure the transmittance of organohydrogels ($30 \times 6 \times 1$ mm³) with a wavelength range from 220 to 1100 nm.

2.5. Mechanical properties

The tensile and compressive properties of the organohydrogels were tested using an electric universal testing system (AGS-X, Shimadzu, Japan) equipped with a 2 kN load cell. Tensile test was conducted using a rectangular sample ($40 \times 10 \times 1$ mm³). Uniaxial compressive test was conducted on a cylindrical shaped sample (10 mm in height, 12 mm in diameter). The loading/unloading of the organohydrogels were tested

using testing system (E42.503, mts, USA) equipped with a 500 N load cell. The rates of the loading/unloading test upon elongation and compression were $10 \text{ mm}\cdot\text{min}^{-1}$ and $2 \text{ mm}\cdot\text{min}^{-1}$, respectively. Cyclic loading–unloading tensile tests were performed to a strain of 300% without intervals between consecutive cycles. Cyclic compressive tests were conducted for ten loading–unloading cycles strain of 50% without intervals between consecutive cycles. The mechanical indexes (tensile strain, tensile stress, Young's modulus, toughness, etc.) were acquired

according to the software [37].

2.6. Ionic conductivity

The ionic conductivity (σ) was studied using a Keithley 6514 system electrometer (TEKTRONIX, INC., USA). The conductivity of the organohydrogel was calculated using the following formula:

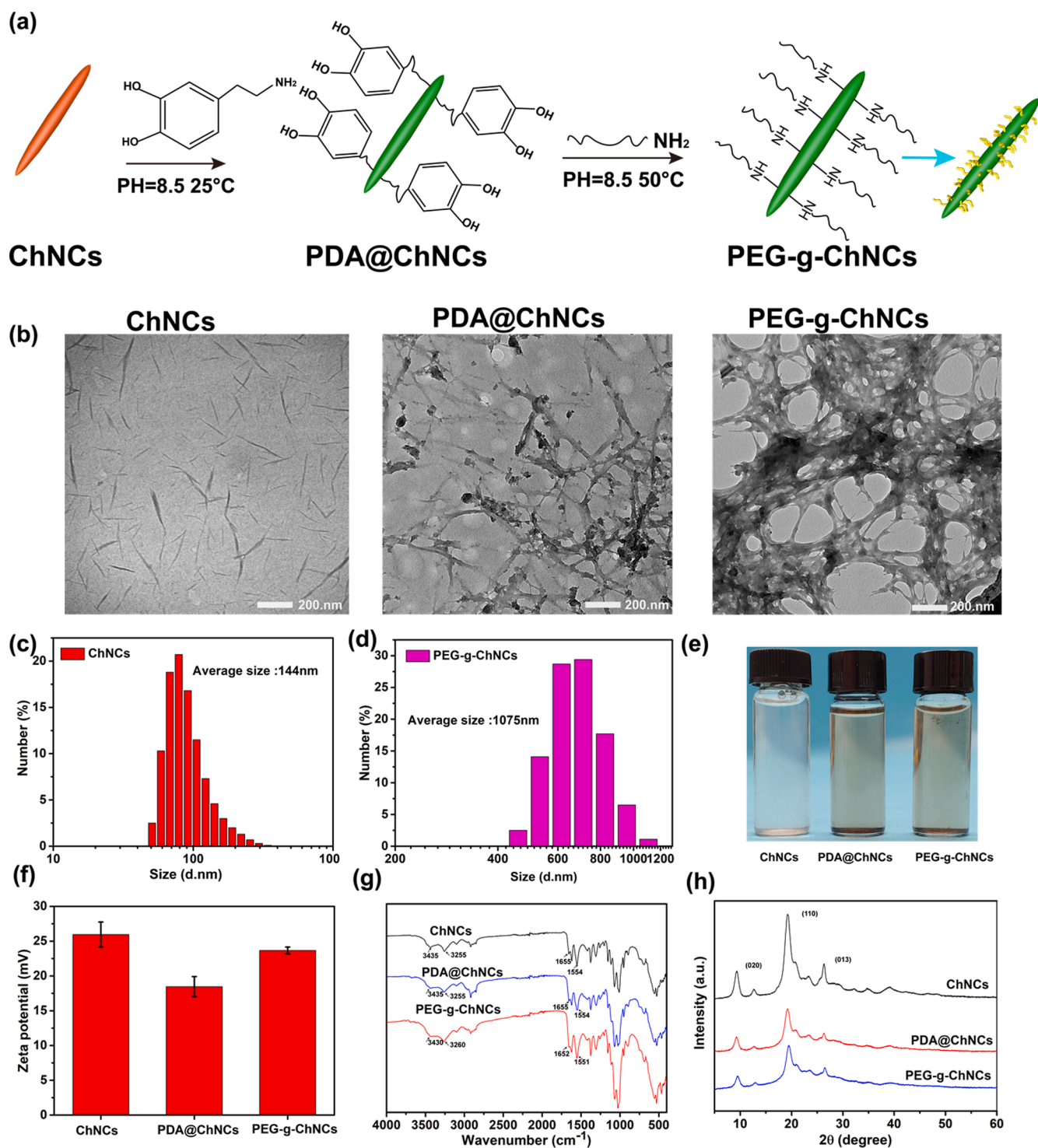


Fig. 1. Schematic diagram showing the surface modification of ChNCs (a); TEM images of ChNCs, PDA@ChNCs, and PEG-g-ChNCs (b); Particle size distribution of ChNCs (c) and PEG-g-ChNCs (d); Photos for the suspension of ChNCs, PDA@ChNCs, and PEG-g-ChNCs in DMSO/H₂O solution maintaining 2 h after sonication (e); Zeta potential (f) FTIR (g) and XRD (h) of ChNCs, PDA@ChNCs and PEG-g-ChNCs.

$$\sigma = \frac{L}{RA} \quad (1)$$

Where, L represents the distance between adjacent electrodes, R represents the resistance of organohydrogel and A represents the contact area of organohydrogels.

Under a variety of temperatures of 25, 10, 0, -20 and -50 °C, the organohydrogel were placed in the insulation foam box for the conductivity measurement. The subzero temperatures were controlled via mixing ethanol and liquid nitrogen with varying ratios.

2.7. Sensor design and testing

PVA/PEG-g-ChNCs organohydrogels were utilized as conductive materials to manufacture strain sensors. Copper wires were connected to the two sides of the PVA/PEG-g-ChNCs organohydrogels sensors as electrodes. The resistance of the PVA/PEG-g-ChNCs organohydrogels sensors were measured using a Keithley 6514 system electrometer after applying a fixed voltage on the sensors. The relative resistance change was calculated by:

$$\text{Relative resistance variations} = \frac{R}{R_0} \quad (2)$$

Where R_0 and R are the resistance without and with applied strain, respectively.

The sensitivity (Gauge factor, GF) under tensile strains was calculated by:

$$GF = \frac{R - R_0}{\varepsilon R_0} \quad (3)$$

Where ε is the axial strain. The sensitivity (S) under compression strains is defined by the slope of resistance change curves.

2.8. Detection of human movement applications

To monitor human movement, the PVA/1%PEG-g-ChNCs organohydrogel was cut into strips of appropriate length, wrapped in 3 M tape to avoid water loss, and attached to different joints of the body, such as the throat, fingers, knees, wrists, and elbows. The wires were clipped on the organohydrogel and connected them to a digital source meter. The change of resistance was calculated by formula (2).

3. Results and discussion

3.1. Characterization of surface functionalization of ChNCs

The surface functionalization process of ChNCs by using PDA as a bridge followed by PEG grafting was shown in Fig. 1a. The PDA layer tightly adhered to the surface of ChNCs through strong hydrogen bonding and van der Waals interactions, and then amino-terminated PEG was chemically bonded to the ChNCs via dehydration reaction [38]. The morphology of ChNCs, PDA@ChNCs, and PEG-g-ChNCs was characterized by TEM (Fig. 1b). ChNCs showed a uniform needle-like nanostructure with a length of 100–500 nm and a width of 15–30 nm. It was observed that the size of ChNCs became slightly larger after PDA modification and further grafting of PEG caused the ChNCs to be physically cross-linked. The morphology result was consistent with the particle size distribution, and the average size of ChNCs, PDA@ChNCs, and PEG-g-ChNCs were 144 nm, 688 nm and 1075 nm for ChNCs, PDA@ChNCs and PEG-g-ChNCs, respectively (Fig. 1c, 1d and Figure S1). Since the ChNCs are non-spherical, the particle size determined by dynamic light scattering was their hydrodynamic radii. Standing for 2 h after ultrasound treatment for 10 min, the suspension of ChNCs can exist stably in DMSO/H₂O solution without aggregation and sedimentation, because of the electrostatic repulsive interaction between positively charged ChNCs. However, after PDA modification and further grafting of

PEG, a little precipitation can be seen in the solution (Fig. 1e). The zeta potential of ChNCs was slightly decreased after grafting PEG (Fig. 1f) since the shielding effect of the polymer chains. In addition, the color of the PDA@ChNCs suspension changed into black due to black PDA particles deposited on the surface of ChNCs. The PEG-g-ChNCs suspension showed similar color with PDA@ChNCs in DMSO/H₂O.

Fig. 1g compared the FTIR spectra of ChNCs, PDA@ChNCs, and PEG-g-ChNCs. The raw ChNCs showed adsorption bands at 3436, 3252, 1655, and 1554 cm^{-1} which were assigned to O–H stretching, N–H stretching, amide I, and amide II, respectively [39]. While the absorption peak of PDA@ChNCs at 3436 cm^{-1} obviously became wider which was associated with an increase in the number of O–H. This result indicated PDA successfully adhered to the surface of the ChNCs. For the PEG-g-ChNCs, the characteristic peaks of ChNCs shifted slightly, and the peak intensity of amide I (1655 cm^{-1}) was evidently decreased as the result of PEG grafting. Compared to the amide I, the peak intensity of amide II almost unchanged, suggesting the ChNCs was partially grafted with PEG. As shown in Fig. 1h, the XRD peaks of ChNCs appeared at 9.6° (020 plane), 19.6° (110 plane), and 26.7° (013 plane) [40]. After modification of PDA, the intensity of the diffraction peaks decreased, and the diffraction peaks of PEG-g-ChNCs were similar to those in PDA@ChNCs pattern. This suggested that PDA and PEG did not change the crystalline structure of ChNCs.

The surface chemical compositions of ChNCs before and after modification were further analyzed using XPS. Figure S2 shows the XPS spectra of ChNCs and PEG-g-ChNCs in the C1s region, and the relative content of carbon-containing functional groups by deconvoluting C1s peaks are shown. The XPS of C1s core-level spectrum for ChNCs can be curve-fitted with three peak components containing binding energies of about 284.8, 286.4, and 287.9 eV, which can be attributed to C–C, C–O/C–N, and C=O species, respectively [41]. After grafting PEG, the intensity of C–C peak components increased obviously. However, due to the shielding effect of PEG on the surface of ChNCs, the intensity of C–O and C–N peaks decreased slightly. The XPS results of PEG grafting on nanoparticles agreed with the previous study [36].

3.2. Synthesis of PVA/PEG-g-ChNCs conductive organohydrogels

Fig. 2a showed the manufacturing process of PVA/PEG-g-ChNCs conductive organohydrogels with mechanical flexibility, fatigue resistance, and freezing-tolerant property. PEG-g-ChNCs was dispersed into DMSO/H₂O binary system, and then mixed with PVA solution. The organohydrogel was obtained by physical crosslinking process of freezing and thawing for one cycle. Finally, the organohydrogel were immersed in salt solution to obtain conductive performance. The good interface compatibility between PVA chains and PEG chains endowed the organohydrogels with excellent mechanical properties while maintaining high conductivity. Hydrogen bonding between PVA matrix and PEG-g-ChNCs played a dominant role in the interfacial interactions of the organohydrogels. In addition, the entanglement of PVA chains and formation of microcrystals in the PVA molecular chain constituted the main network structure of hydrogels. In this system, DMSO can promote the gelation of PVA and apparently enhance the mechanical properties of the organohydrogels. DMSO molecules can form hydrogen bond with water at 1:2 ratio giving a stable six-ring configuration, which inhibits the formation of ice crystals.[11] The interaction between DMSO and water gave the organohydrogel a property of anti-freezing at sub-zero temperature.

As shown in Fig. 2b, the cross section image of SEM of pure PVA organohydrogel was smooth. After adding PEG-g-ChNCs, the section of the organohydrogel was much rougher. It was obvious that rod-like PEG-g-ChNCs was embedded in PVA matrix with many “brush” attached to PVA. It is interesting that no pore structure can be identified in all sample which is different from that of the free-dried hydrogel. This can be understood by that no ice crystals in the organohydrogel were formed during freezing process, since the organohydrogel has high low-

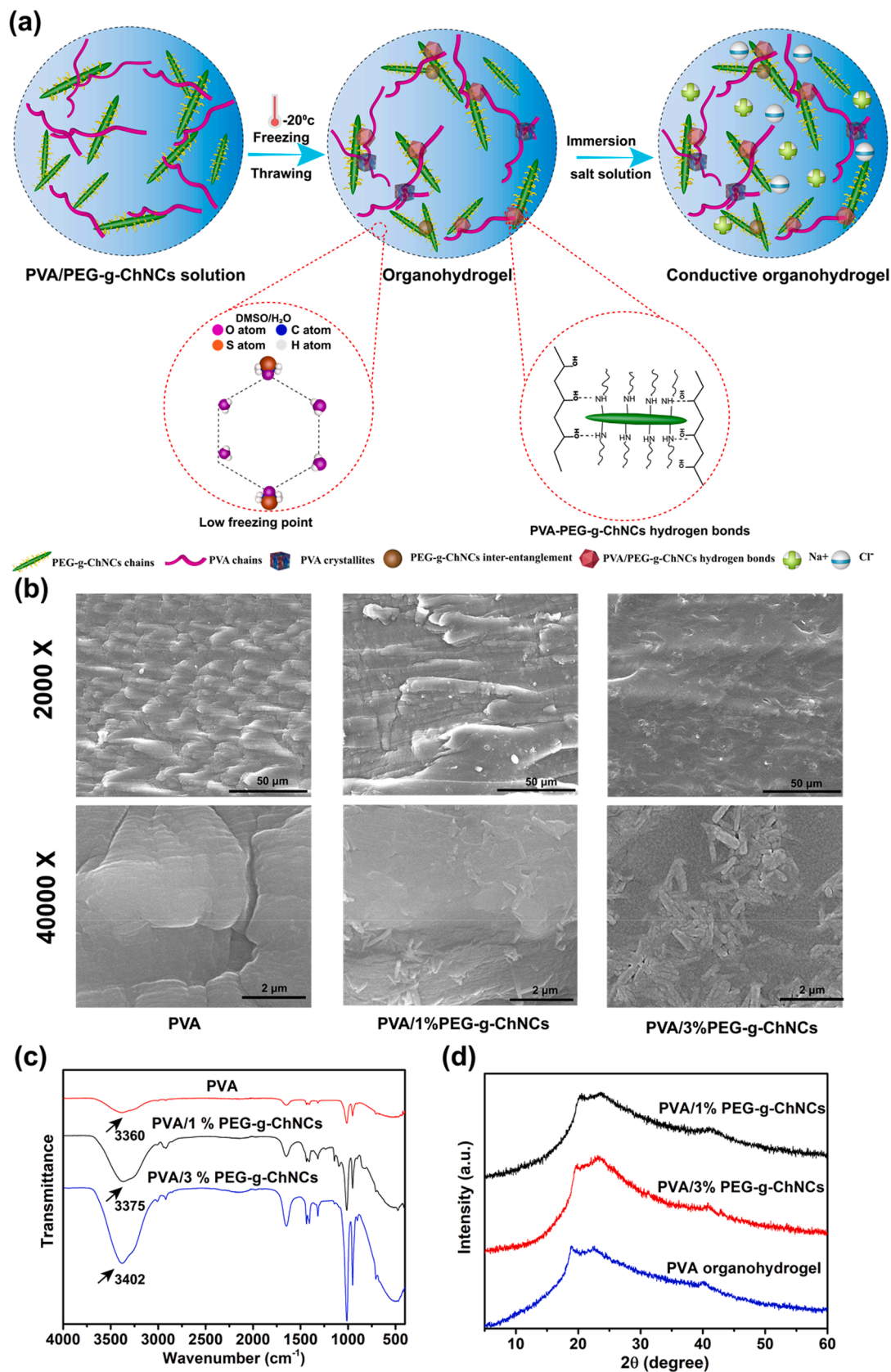


Fig. 2. Schematic diagram of formation process of PVA/PEG-g-ChNCs conductive organohydrogel (a); SEM images (b); FTIR spectra (c); XRD pattern (d) of PVA and PVA/PEG-g-ChNCs organohydrogels.

temperature resistant property. To further characterize the interactions between PEG-g-ChNCs and PVA matrix, PVA organohydrogel, PVA/1% PEG-g-ChNCs organohydrogel and PVA/3%PEG-g-ChNCs organohydrogel were monitored by FTIR spectra (Fig. 2c). The characteristic absorption peak of PVA/PEG-g-ChNCs organohydrogel around 3300 cm^{-1} corresponds to the stretching vibration of -OH groups. The intensity of this absorption peak reflects the number of hydrogen bonds. With the addition of PEG-ChNCs, the characteristic stretching band of -OH obviously broadened, indicating that PEG-g-ChNCs increased the number of hydrogen bonds and enhanced the hydrogen bond interactions in organohydrogel. The XRD of PVA organohydrogel, PVA/PEG-g-ChNCs organohydrogels was then conducted (Fig. 2d). As for PVA organohydrogel, the characteristic peaks appeared at 18.8° , 22.4° and 40.0° corresponding to (1 0 1), (2 0 0) and (1 1 1) planes of crystals for PVA [42]. The diffraction peaks of PVA/PEG-g-ChNCs organohydrogels were the same as PVA hydrogel and no peaks of ChNCs can be identified due to the small amount of the ChNCs in PVA matrix. PVA/1% PEG-g-ChNCs organohydrogel shows good transparency. The transmittance at 800 nm wavelengths was close to 60% (Figure S3). This high transparency was obtained by quenching PVA DMSO/ H_2O solution to initiate sol-gel transition at -20°C . By quenching at low temperature, the phase separation of PVA is greatly restricted. The PVA chain can be crystallized uniformly in the system to form smaller crystallites, thus reducing the interference to visible light. With the increase of PEG-g-ChNCs content, the transmittance decreased sharply, and reached 28% at 800 nm wavelength at 3% PEG-g-ChNCs content. The decrease in transmittance may be due to light scattering caused by the added PEG-g-ChNCs.

3.3. Mechanical properties of PVA/PEG-g-ChNCs organohydrogels

The mechanical properties of hydrogels, such as strength, toughness and durability, are the extremely important in application in flexible sensor. The PVA/PEG-g-ChNCs organohydrogel showed excellent mechanical properties, which can withstand various deformations, such as, cyclic twisting, folding and bending (Video S1). It is worth noting that the PVA/PEG-g-ChNCs organohydrogel can be stretched to almost five times of its original length without breaking (Fig. 3a). Moreover, the composite organohydrogels maintained a good self-recovery ability when it be compressed under constant cracking (Fig. 3b). The PVA/PEG-g-ChNCs can withstand 1.2 kg of weight (Fig. 3c), and it was stretched to a certain length with no break in the case of knotting (Fig. 3d). Fig. 3e shows that the PVA/PEG-g-ChNCs organohydrogel also displayed excellent puncture resistance.

In order to systematically investigate the influence of PEG-g-ChNCs on the mechanical properties of the organohydrogels, tensile and compression tests were conducted, a typical tensile stress-strain curve of the prepared organohydrogel was shown in Fig. 3f. The tensile strength and elongation at break of all organohydrogels containing ChNCs increased compared with PVA organohydrogel. Obviously, the organohydrogels with the PEG-g-ChNCs had a significantly better enhancement than adding raw ChNCs. This may be due to uneven stress distribution caused by agglomeration of unmodified ChNCs in polymer matrix and the poor interfacial adhesion between ChNCs and PVA. On the contrary, the organohydrogels containing PEG-g-ChNCs exhibited improved mechanical properties. With the increase of PEG-g-ChNCs content from 1% to 3%, the tensile strength increased monotonically from nearly 1.5 to 2.0 MPa (Fig. 3g), and the fracture strain increased from 345% to 435% (Fig. 3h). The maximum tensile strength of PVA/PEG-g-ChNCs organohydrogel was about 2 times that of PVA organohydrogel, and the toughness increased from 3.1 MJ/m^3 to 4.7 MJ/m^3 . On the other hand, the compressive strength of PVA/PEG-g-ChNCs increased from 4.5 to 8.8 MPa at 80% strain (Figure S4a) with the increase of PEG-g-ChNCs content from 1% to 3%. Such excellent mechanical properties were attributed to the synergistic effect of DMSO/ H_2O binary solvent system of PVA organohydrogel and the good compatibility of between PEG-g-

ChNCs and PVA matrix. Previous studies have shown that the most flexible PVA organohydrogel can be obtained at a weight ratio of 3:2 of DMSO/ H_2O (1:3 M ratio), and DMSO formed hydrogen bonds with water at a molar ratio of 1:2, [11] which can limit their hydrogen bonding to the PVA molecular chain. Therefore, there were large number of PVA crystallization regions acting as crosslinking points which helped to strengthen the PVA. Besides, the interfacial interactions between PVA chains and PEG-g-ChNCs via forming hydrogen bonds played a key role in enhancing the organohydrogel. When an external force was applied to the organohydrogel, stress can be effectively transferred to the flexible PEG-g-ChNCs, resulting in the rearrangement of PEG-g-ChNCs in the direction of applied stress.

Fig. 3i shows the PVA/1%PEG-g-ChNCs organohydrogel dissipate energy during tension resulting in a large lag, which contributed to the generation of hydrogen bonding and electrostatic interactions through destruction and reassembly. The lag per unit volume of PVA/1%PEG-g-ChNCs organohydrogel increased from 0.16 MJ/m^3 at 25% strain to 1.65 MJ/m^3 at 300% strain (Fig. 3j). In addition, the dissipation coefficient increased with the set strain, indicating that the prepared PVA/PEG-g-ChNCs organohydrogel can effectively dissipate energy under large deformation. A higher energy loss factor of 54% can be observed during the first compression cycle (Figure S4b), indicating a breakage of covalent bonds in the gel network. After 10 cycles of compression to 50% strain, PVA/1%PEG-g-ChNCs organohydrogel can still recover to their original shape without significant attenuation of the ultimate stress (Fig. 3k). The hysteresis loops of cycles 2-10th kept almost overlap, indicating that the damaged physical crosslinking can be partially recovered quickly. In short, the organohydrogel has excellent shape recovery properties due to the flexible network structure and nano reinforcing effect.

3.4. Freezing-tolerant and moisturizing properties of the PVA/PEG-g-ChNCs organohydrogel.

In general, the sensor properties based on hydrogels are easily affected by temperature especially at low temperature environment, since the solvents in hydrogels would be frozen, causing them to harden and lose their functions. Therefore, it is important to develop organohydrogels that can work in low temperature environments. To study the freezing-tolerant properties of PVA/PEG-g-ChNCs organohydrogels, the sample was frozen for 12 h at -20°C before the experiment and kept cold during the test. PVA hydrogels harden at -20°C and was completely frozen and easily destroyed by twisting at -50°C , while PVA/1%PEG-g-ChNCs organohydrogel can be twisted and bent without breaking and maintain good flexibility, which indicated that the organohydrogels had excellent freezing-tolerant properties (Fig. 4a). This was attributed to binary DMSO/ H_2O solvent, in which DMSO molecule can form hydrogen bonds with water as discussed above, which inhibited the formation of ice crystals at temperatures below zero and gave the freezing-tolerant properties of PVA/1%PEG-g-ChNCs organohydrogel.

Normally, hydrogels are easy to lose water when they exposed to air, resulting in loss of flexible performance. Therefore, improving the long-term stability of hydrogels is of practical significance for hydrogel-based sensors. The weight changes of PVA/1%PEG-g-ChNCs and PVA organohydrogels at 25°C for 15 days were recorded and the result was shown in Fig. 4b. Because of the large amount of free water in the PVA hydrogel solvent, the weight loss of PVA hydrogel during the first 4 days was significant. However, when the solvent was DMSO/ H_2O , the weight loss was relatively slow, this result was attributed to the interactions between DMSO and water prevented water from evaporating.

In order to obtain the conductive behavior of hydrogels, a large number of migratory Na^+ and Cl^- ions were incorporated by immersing the organohydrogels in different concentrations of NaCl solutions (Figure S5). With the increase of NaCl concentration to 1 M, the ionic conductivity of all organohydrogels increased by about 10 times, due to

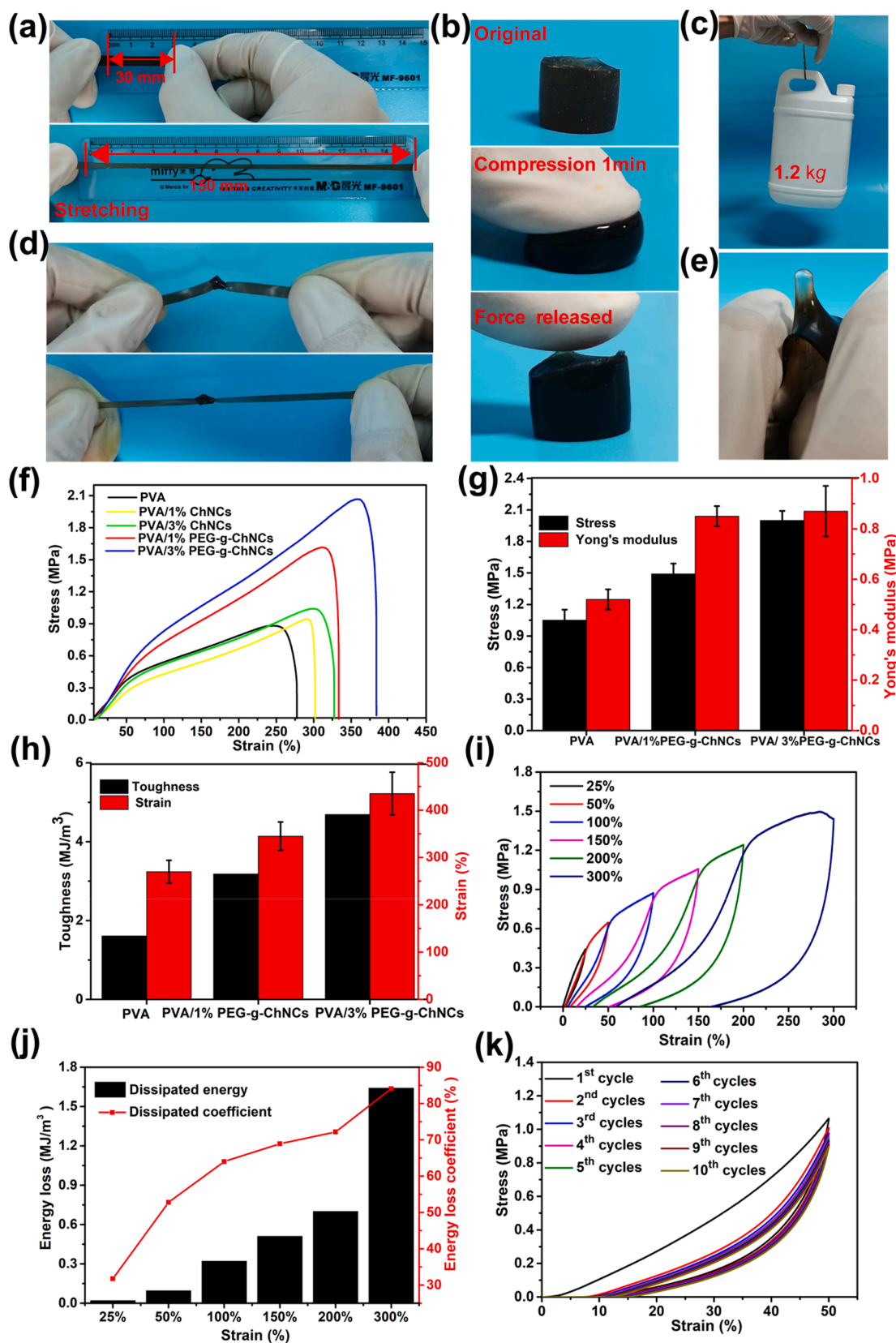


Fig. 3. Mechanical properties of the PVA/PEG-g-ChNCs organohydrogels: the organohydrogel can be stretched (a), compressed (b), lift weight (c), twisted and stretched with knot (d); Puncture resistance of the organohydrogel by a miniature glass rod (e); Typical tensile stress–strain curves (f); Stress and Young’s modulus values (g); Strain and toughness values (h) of PVA/PEG-g-ChNCs organohydrogels; Loading–unloading measurement of the PVA/1%PEG-g-ChNCs organohydrogel under varied strains without a resting interval (i); Calculated dissipated energy and the energy loss coefficient of the PVA/1%PEG-g-ChNCs organohydrogel during the loading–unloading tests under different strains (j); Cyclic compressive stress–strain curves of PVA/1%PEG-g-ChNCs organohydrogel (k).

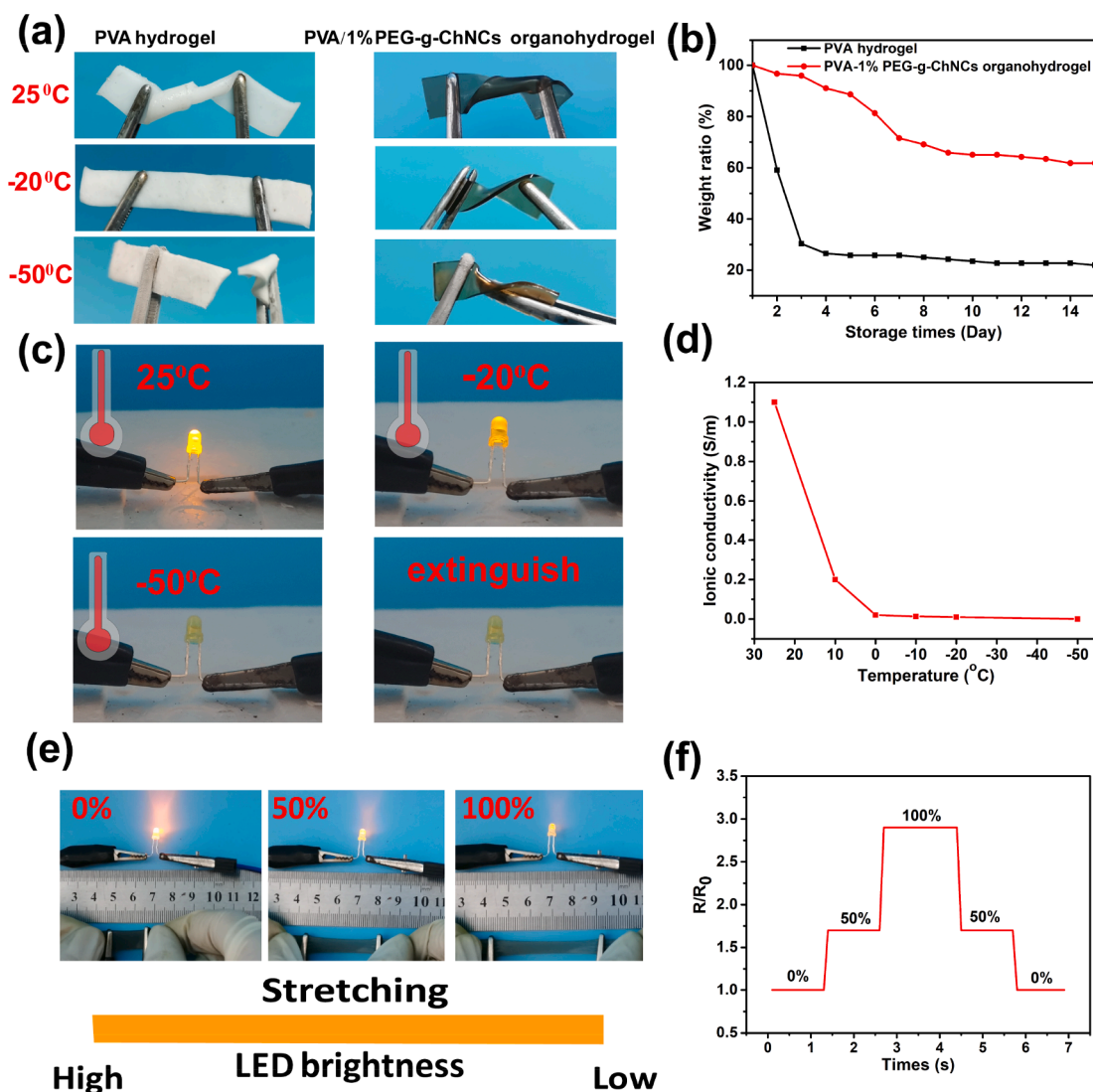


Fig. 4. Freezing tolerance behaviors of PVA and PVA/1%PEG-g-ChNCs hydrogels (a); Weight variation ratio of the hydrogels under 50% relative humidity at 25 °C (b); Comparisons of luminance of LEDs (working voltage of 3.6 V) by using PVA/1%PEG-g-ChNCs organohydrogel as conductor at varying temperature (c); Ionic conductivity of PVA/1%PEG-g-ChNCs organohydrogels at 25 °C to –50 °C (d); The changes of LED brightness by stretching with strain at 0%, 50% and 100% (e); The variation of the relative resistance along with strain at 0%, 50% and 100% (f).

the dissociated ions concentration increased at higher salt concentrations. However, when NaCl concentration was further increased to 2 M, the measured ionic conductivity was similar to that of 1 M. The constant ionic conductivity at higher NaCl concentration indicated that the cumulated ion mobility did not change. As further increased ion concentration, excessive charge carriers formed ion pairs or clusters instead of being maintained as dissociated ions, thus contributing little to the ion conductivity.[43] The ionic conductivity of PVA/1% PEG-g-ChNCs organohydrogel was demonstrated by illuminating the LED at a various temperature as a conductor in the circuit (Fig. 4c). The brightness of LED became weaker with decreasing temperature, confirming the reduced ionic conductivity at lower temperature. It was worth noting that this LED can emit a weak light at –20 °C, which verified the possibility use of the organohydrogel at low temperature. The conductivity of organohydrogels was affected by temperature as shown in Fig. 4d. With the decrease of temperature, the ionic conductivity decreased from 1.15 to 0.01 S/m, while the decrease of ionic conductivity at lower temperature can be attributed to slower and limited ionic mobility when temperature was declined. After soaking in salt solution, the strain sensing of the PVA/1%PEG-g-ChNCs organohydrogel was tested by application of it in a complete circuit connecting a LED lamp

(Fig. 4e). When the organohydrogel was stretched from 0% to 100%, the brightness of LED decreased synchronously, indicating that the ionic conductivity of PVA/1%PEG-g-ChNCs organohydrogel was sensitively affected by deformation (Video S2). This was due to the extended ion transport pathway, resulting in resistance increase and brightness reduction. Fig. 6f showed the change in relative resistance as a function of strain. The result showed that the relative resistance exhibited a trend with stepwise tensile cycling by applying 50% and 100% tensile strains. This also demonstrated the feasibility of using stretchable conductive organohydrogels as wearable strain sensors.

3.5. Sensing performance of the PVA/PEG-g-ChNCs organohydrogels

The good comprehensive properties of PVA/1% PEG-g-ChNCs organohydrogels, including electrical conductivity, light transmittance, toughness, anti-freezing and moisture retention, makes them become a promising candidate for resistance sensors. The sensitivity and reliability under both stretching and compressive deformation were presented in Fig. 5a. The relative resistance of PVA/1%PEG-g-ChNCs organohydrogel increased with the increase of strain, indicating linear piezoresistive behavior for tensile strain (Fig. 5b). Normally, for

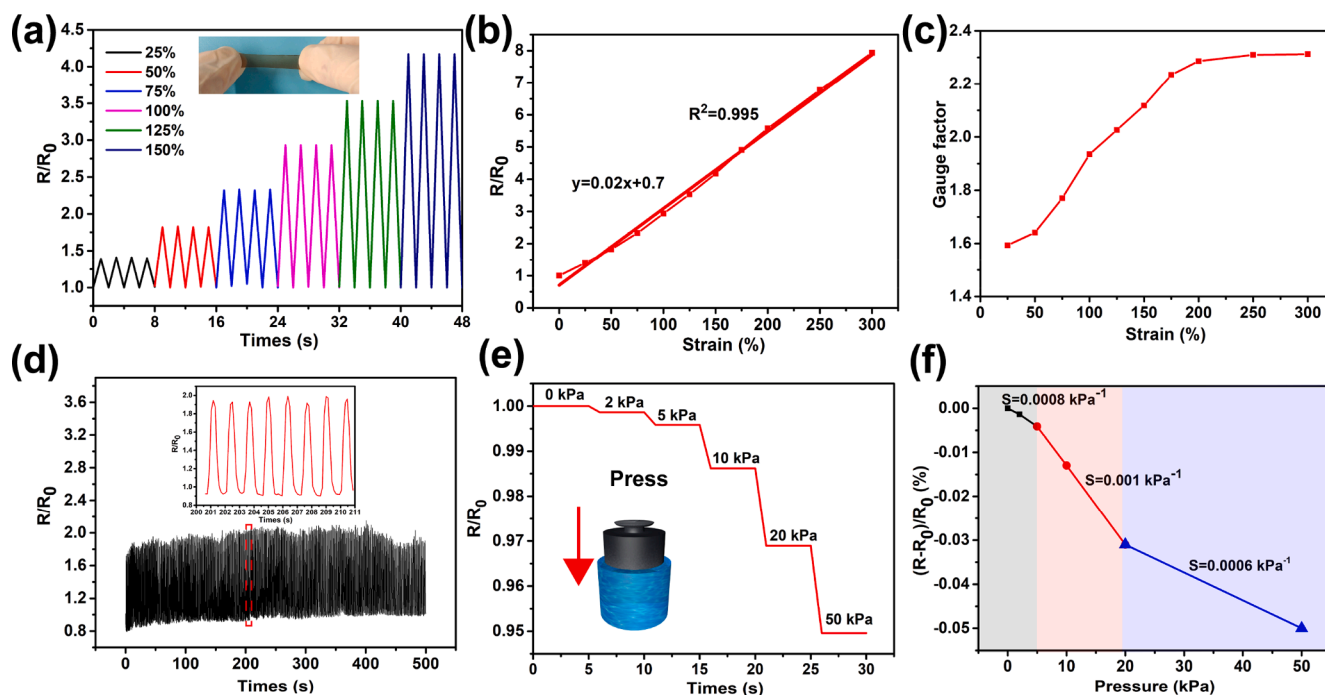


Fig. 5. Sensitive sensing performance of the PVA/1%PEG-g-ChNCs organohydrogel sensor: Time-dependent relative resistance change of the sensor with different tensile strains (a); Relative resistance change with the increase of tensile strain (b); The effects of various applied strains on the gauge factor (c); Relative resistance change under cyclic stretching-releasing test for up to 600 cycles at 50% tensile strain (d); Time profile of the relative resistance change with applied pressure (e); Relative resistance change and pressure sensitivity of PVA/1%PEG-g-ChNCs organohydrogels-based sensor at varying pressure (f).

hydrogel-based strain sensors, the conductive path affected by plastic deformation increased in a nonlinear exponential dependence of sensitivity with increasing strain, which was deviated from linearity under large deformation. Notably, the strain sensor not only had a high linear relationship between 0 and 300% ($R^2 = 0.995$), but also had a high sensitivity of GF of 2.3 (Fig. 5c). In addition, the durability and repeatability of the sensor were also further studied. The sensor used a 50% load-unload process for 600 cycles, and the magnification illustration in Fig. 5d showed the stability and linear variation of the output resistance signal. It can be observed that there was little attenuation in the variation of resistance, indicating excellent stability and durability. Only negligible electrical hysteresis may be related to the destruction and reconstruction of the conductive network structure. The excellent compression elasticity of PVA/1%PEG-g-ChNCs organohydrogel made it an ideal choice for pressure sensor to detect compression stimulus. In contrary to strain sensing behavior, a decrease in resistance can be observed as the compression pressure increased continuously due to shorter ion transport paths (Fig. 5e). The pressure sensitivity of the pressure sensor represents the slope of the change in relative resistance under the varying pressure curve, that is, the rate of change in resistance relative to the pressure [44]. Similar to other types of pressure sensors, the sensitivity of the PVA/1%PEG-g-ChNCs organohydrogel sensor was divided into several zones. Sensitivity was 0.0008 kPa^{-1} and 0.001 kPa^{-1} within the pressure range of 0–5 and 5–20 kPa, respectively. The sensitivity of the organohydrogel sensor decreased to 0.0006 kPa^{-1} when the applied pressure exceeded 20 kPa (Fig. 5f).

3.6. Real-Life demonstration as wearable sensors

The outstanding features of the synthesized organohydrogel-based strain sensor make it possible to use as a wearable electronic device to accurately identify real-time subtle human physiological signals and human movements. As shown in Fig. 6a, an organohydrogel strain sensor was mounted on a volunteer's throat to monitor complex cuticular movement and vibration. Relative change curves showed similar

and stable response peaks when the volunteers swallowed repeatedly. The organohydrogel sensor was used to sensitively detect different joint movements, the differences in frequency resistance signal curves could be attributed to the changed speed of bending and degree of distortion. The organohydrogel sensor was then connected to the neck and elbow (Fig. 6b and c), and the motion signals produced by different joint movements were different. Therefore, the organohydrogel strain sensor can clearly distinguish the various bending behaviors of the joint. Fig. 6d showed the relative resistance change of the organohydrogel sensor with inspiration/expiration. It also showed high sensitivity and repeatability. The organohydrogel sensor can also be used to detect the motion signal of the knee in a state of standing and walking (Fig. 6e). Finger bends at different angles can be accurately reflected by changes in relative resistance (Fig. 6f). At different bending angles of 30, 60 and 90°, the relative resistance of the organohydrogel increased with the increase of the bending angle, and the resistance value remained constant while the finger was at a certain angle. Besides, pressure sensors based on organohydrogel can also be used for sensory motion detection (Figure S6). Sensitive and stable detection capabilities make PVA/PEG-g-ChNCs organohydrogel sensor being a powerful competitor for flexible wearable sensor.

4. Conclusions

Ionic conductive organohydrogel composed with PVA and PEG-g-ChNCs with stretchable and anti-freezing properties were prepared through freezing/thawing and using DMSO/water solvent. The surface of ChNCs was grafted with PEG polymer, and the grafted ChNCs exhibited excellent compatibility with PVA matrix. The interaction between PEG and PVA solved the dispersion problem of PEG-g-ChNCs in the matrix and led to the high strength (2.0 MPa) of organohydrogel which was superior to that of the original organohydrogel (0.85 MPa). Moreover, the usage of DMSO gave the organohydrogel long-term moisturizing performance. The conductive organohydrogels were then prepared by immersing in salt solution, and it showed high sensitivity

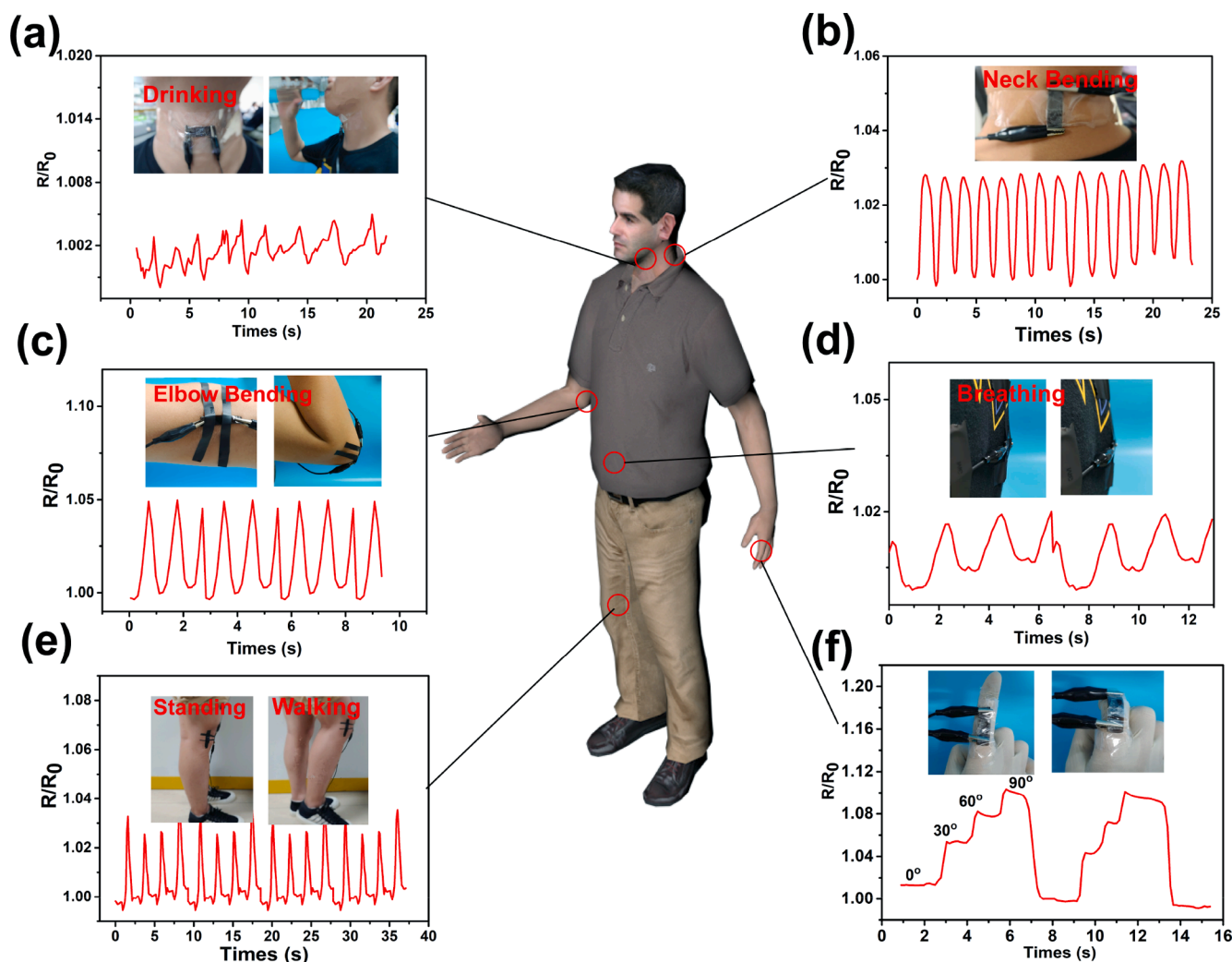


Fig. 6. Relative resistance variations of the PVA/1%PEG-g-ChNCs organohydrogel sensor attached to the throat (a), neck (b), elbow (c), abdomen (d), knee (e) and finger (f).

and stability in monitoring human activities. This work has developed a simple method to prepare a superelastic, tough, anti-freezing and conductive organohydrogel, which shows great potential as wearable devices.

CRediT authorship contribution statement

Jiabi Cai: Validation, Formal analysis, Investigation, Data curation, Writing – original draft. **Yunqing He:** Methodology. **Youquan Zhou:** Software, Investigation. **Hongbo Yu:** Investigation. **Binghong Luo:** Resources. **Mingxian Liu:** Conceptualization, Methodology, Supervision, Writing – review & editing.

Declaration of Competing Interest

The authors declare that they have no known competing financial interests or personal relationships that could have appeared to influence the work reported in this paper.

Acknowledgements

This work was financially supported by the National Natural Science Foundation of China (52073121), Natural Science Foundation of Guangdong Province (2019A1515011509), Science and Technology Planning Project of Guangzhou (202102010117), and the Fundamental

Research Funds for the Central Universities (21619102).

Appendix A. Supplementary material

Supplementary data to this article can be found online at <https://doi.org/10.1016/j.compositesa.2022.106813>.

References

- [1] Wang J, Lin M-F, Park S, Lee PS. Deformable conductors for human-machine interface. *Mater Today* 2018;21(5):508–26.
- [2] Liao H, Guo X, Wan P, Yu G. Conductive MXene nanocomposite organohydrogel for flexible, healable, low-temperature tolerant strain sensors. *Adv Funct Mater* 2019;29(39):1904507.
- [3] Han L, Lu X, Liu K, Wang K, Fang L, Weng L-T, et al. Mussel-inspired adhesive and tough hydrogel based on nanoclay confined dopamine polymerization. *ACS Nano* 2017;11(3):2561–74.
- [4] Shin SR, Jung SM, Zalabany M, Kim K, Zorlutuna P, Sb K, et al. Carbon-nanotube-embedded hydrogel sheets for engineering cardiac constructs and bioactuators. *ACS Nano* 2013;7(3):2369–80.
- [5] Wang C, Hwang D, Yu Z, Takei K, Park J, Chen T, et al. User-interactive electronic skin for instantaneous pressure visualization. *Nat Mater* 2013;12(10):899–904.
- [6] Darabi MA, Khosrozadeh A, Mbeleck R, Liu Y, Chang Q, Jiang J, et al. Skin-inspired multifunctional autonomic-intrinsic conductive self-healing hydrogels with pressure sensitivity, stretchability, and 3D printability. *Adv Mater* 2017;29(31):1700533.
- [7] Keplinger C, Sun J-Y, Foo CC, Rothmund P, Whitesides GM, Suo Z. Stretchable, transparent, ionic conductors. *Science* 2013;341(6149):984–7.

- [8] Wang C, Li X, Gao E, Jian M, Xia K, Wang Q, et al. Carbonized silk fabric for ultrastretchable, highly sensitive, and wearable strain sensors. *Adv Mater* 2016;28(31):6640–8.
- [9] Jiang S, Liu S, Feng W. PVA hydrogel properties for biomedical application. *J Mech Behav Biomed Mater* 2011;4(7):1228–33.
- [10] Teodorescu M, Bercea M, Morariu S. Biomaterials of PVA and PVP in medical and pharmaceutical applications: Perspectives and challenges. *Biotechnol Adv* 2019;37(1):109–31.
- [11] Ye Y, Zhang Y, Chen Y, Han X, Jiang F. Cellulose nanofibrils enhanced, strong, stretchable, freezing-tolerant ionic conductive organohydrogel for multi-functional sensors. *Adv Funct Mater* 2020;30(35):2003430.
- [12] Bian H, Jiao L, Wang R, Wang X, Zhu W, Dai H. Lignin nanoparticles as nano-spacers for tuning the viscoelasticity of cellulose nanofibril reinforced polyvinyl alcohol-borax hydrogel. *Eur Polym J* 2018;107:267–74.
- [13] Yang Y, Wang X, Yang F, Wang L, Wu D. Highly elastic and ultratough hybrid ionic-covalent hydrogels with tunable structures and mechanics. *Adv Mater* 2018;30(18):1707071.
- [14] Qin Z, Dong D, Yao M, Yu Q, Sun X, Guo Q, et al. Freezing-tolerant supramolecular organohydrogel with high toughness, thermoplasticity, and healable and adhesive properties. *ACS Appl Mater Interfaces* 2019;11(23):21184–93.
- [15] Sun X, Qin Z, Ye L, Zhang H, Yu Q, Wu X, et al. Carbon nanotubes reinforced hydrogel as flexible strain sensor with high stretchability and mechanically toughness. *Chem Eng J* 2020;382:122832.
- [16] Ma C, Le X, Tang X, He J, Xiao P, Zheng J, et al. A multiresponsive anisotropic hydrogel with macroscopic 3D complex deformations. *Adv Funct Mater* 2016;26(47):8670–6.
- [17] Zhu F, Zheng SY, Lin J, Wu ZL, Yin J, Qian J, et al. Integrated multifunctional flexible electronics based on tough supramolecular hydrogels with patterned silver nanowires. *J Mater Chem C* 2020;8(23):7688–97.
- [18] Gao Y, Peng J, Zhou M, Yang Y, Wang X, Wang J, et al. A multi-model, large range and anti-freezing sensor based on a multi-crosslinked poly (vinyl alcohol) hydrogel for human-motion monitoring. *J Mater Chem B* 2020;8(48):11010–20.
- [19] Wang Z, Cong Y, Fu J. Stretchable and tough conductive hydrogels for flexible pressure and strain sensors. *J Mater Chem B* 2020;8(16):3437–59.
- [20] Yang C, Suo Z. Hydrogel ionotronics. *Nat. Rev. Mater.* 2018;3:125–42.
- [21] Gu J, Huang J, Chen G, Hou L, Zhang J, Zhang X, et al. Multifunctional Poly (vinyl alcohol) Nanocomposite Organohydrogel for Flexible Strain and Temperature Sensor. *ACS Appl Mater Interfaces* 2020;12(36):40815–27.
- [22] Zeng J-B, He Y-S, Li S-L, Wang Y-Z. Chitin whiskers: An overview. *Biomacromolecules* 2012;13(1):1–11.
- [23] Kumar MR. Chitin and chitosan fibres: a review. *Bull Mater Sci* 1999;22(5):905.
- [24] Ou X, Yang X, Zheng J, Liu M. Free-standing graphene oxide–chitin nanocrystal composite membrane for dye adsorption and oil/water separation. *ACS Sustainable Chem Eng* 2019;7(15):13379–90.
- [25] Ou X, Cai J, Tian J, Luo B, Liu M. Superamphiphobic surfaces with self-cleaning and antifouling properties by functionalized chitin nanocrystals. *ACS Sustainable Chem Eng* 2020;8(17):6690–9.
- [26] Rosso P, Ye L, Friedrich K, Sprenger S. A toughened epoxy resin by silica nanoparticle reinforcement. *J Appl Polym Sci* 2006;100(3):1849–55.
- [27] Carballera P, Hauptert F. Toughening effects of titanium dioxide nanoparticles on TiO₂/epoxy resin nanocomposites. *Polym Compos* 2010;31(7):1241–6.
- [28] Araki J, Kurihara M. Preparation of sterically stabilized chitin nanowhisker dispersions by grafting of poly (ethylene glycol) and evaluation of their dispersion stability. *Biomacromolecules* 2015;16(1):379–88.
- [29] Ifuku S, Iwasaki M, Morimoto M, Saimoto H. Graft polymerization of acrylic acid onto chitin nanofiber to improve dispersibility in basic water. *Carbohydr Polym* 2012;90(1):623–7.
- [30] Li C, Liu H, Luo B, Wen W, He L, Liu M, et al. Nanocomposites of poly (l-lactide) and surface-modified chitin whiskers with improved mechanical properties and cytocompatibility. *Eur Polym J* 2016;81:266–83.
- [31] Liu H, Wang X, Cao Y, Yang Y, Yang Y, Gao Y, et al. Freezing-tolerant, highly sensitive strain and pressure sensors assembled from ionic conductive hydrogels with dynamic cross-links. *ACS Appl Mater Interfaces* 2020;12(22):25334–44.
- [32] Wu J, Wu Z, Lu X, Han S, Yang B-R, Gui X, et al. Ultrastretchable and stable strain sensors based on antifreezing and self-healing ionic organohydrogels for human motion monitoring. *ACS Appl Mater Interfaces* 2019;11(9):9405–14.
- [33] Lu C, Chen X. All-temperature flexible supercapacitors enabled by antifreezing and thermally stable hydrogel electrolyte. *Nano Lett* 2020;20(3):1907–14.
- [34] Yang L-J, Yang X-Q, Huang K-M, Jia G-Z, Shang H. Dielectric properties of binary solvent mixtures of dimethyl sulfoxide with water. *Int. J. Mol. Sci.* 2009;10:1261–70.
- [35] Revol J-F, Marchessault R. In vitro chiral nematic ordering of chitin crystallites. *Int J Biol Macromol* 1993;15(6):329–35.
- [36] Li L, Bao R-Y, Gao T, Liu Z-Y, Xie B-H, Yang M-B, et al. Dopamine-induced functionalization of cellulose nanocrystals with polyethylene glycol towards poly (L-lactic acid) bionanocomposites for green packaging. *Carbohydr Polym* 2019;203:275–84.
- [37] Di X, Ma Q, Xu Y, Yang M, Wu G, Sun P. High-performance ionic conductive poly (vinyl alcohol) hydrogels for flexible strain sensors based on a universal soaking strategy. *Mater Chem Front* 2021;5(1):315–23.
- [38] Yang J, Qi G-Q, Tang L-S, Bao R-Y, Bai L, Liu Z-Y, et al. Novel photodriven composite phase change materials with bioinspired modification of BN for solar-thermal energy conversion and storage. *J Mater Chem A* 2016;4(24):9625–34.
- [39] Lin N, Zhao S, Gan L, Chang PR, Xia T, Huang J. Preparation of fungus-derived chitin nanocrystals and their dispersion stability evaluation in aqueous media. *Carbohydr Polym* 2017;173:610–8.
- [40] Zhao X, Su Y, Liu Y, Li Y, Jiang Z. Free-standing graphene oxide-palygorskite nanohybrid membrane for oil/water separation. *ACS Appl Mater Interfaces* 2016;8(12):8247–56.
- [41] Zhao C, Zhang Z, Liu Y, Shang N, Wang HJ, Wang C, et al. Palladium nanoparticles anchored on sustainable chitin for phenol hydrogenation to cyclohexanone. *ACS Sustainable Chem Eng* 2020;8(32):12304–12.
- [42] Dai H, Huang Y, Huang H. Eco-friendly polyvinyl alcohol/carboxymethyl cellulose hydrogels reinforced with graphene oxide and bentonite for enhanced adsorption of methylene blue. *Carbohydr Polym* 2018;185:1–11.
- [43] Chen AA, Pappu RV. Quantitative characterization of ion pairing and cluster formation in strong 1: 1 electrolytes. *J Phys Chem B* 2007;111(23):6469–78.
- [44] Yang Y, Yang Y, Cao Y, Wang X, Chen Y, Liu H, et al. Anti-freezing, resilient and tough hydrogels for sensitive and large-range strain and pressure sensors. *Chem Eng J* 2021;403:126431.

Support Information

Polyethylene glycol grafted chitin nanocrystals enhanced, stretchable, freezing-tolerant ionic conductive organohydrogel for strain sensors

Jiabin Cai^a, Yunqing He^a, Youquan Zhou^a, Hongbo Yu^a, Binghong Luo^a, Mingxian Liu^{a,*}

^aDepartment of Materials Science and Engineering, College of Chemistry and Materials Science,

Jinan University, Guangzhou 510632, China

*Corresponding author. Email: liumx@jnu.edu.cn

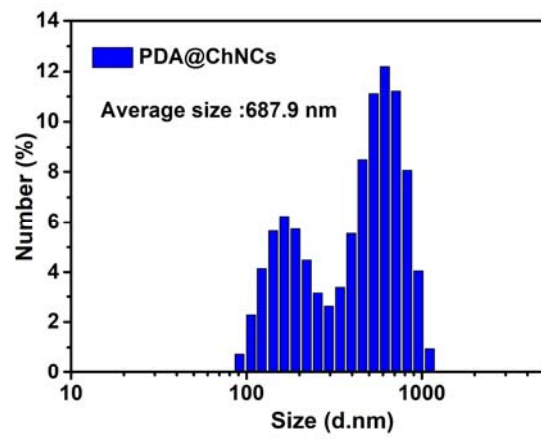


Figure S1. Particle size distribution of PDA@ChNCs.

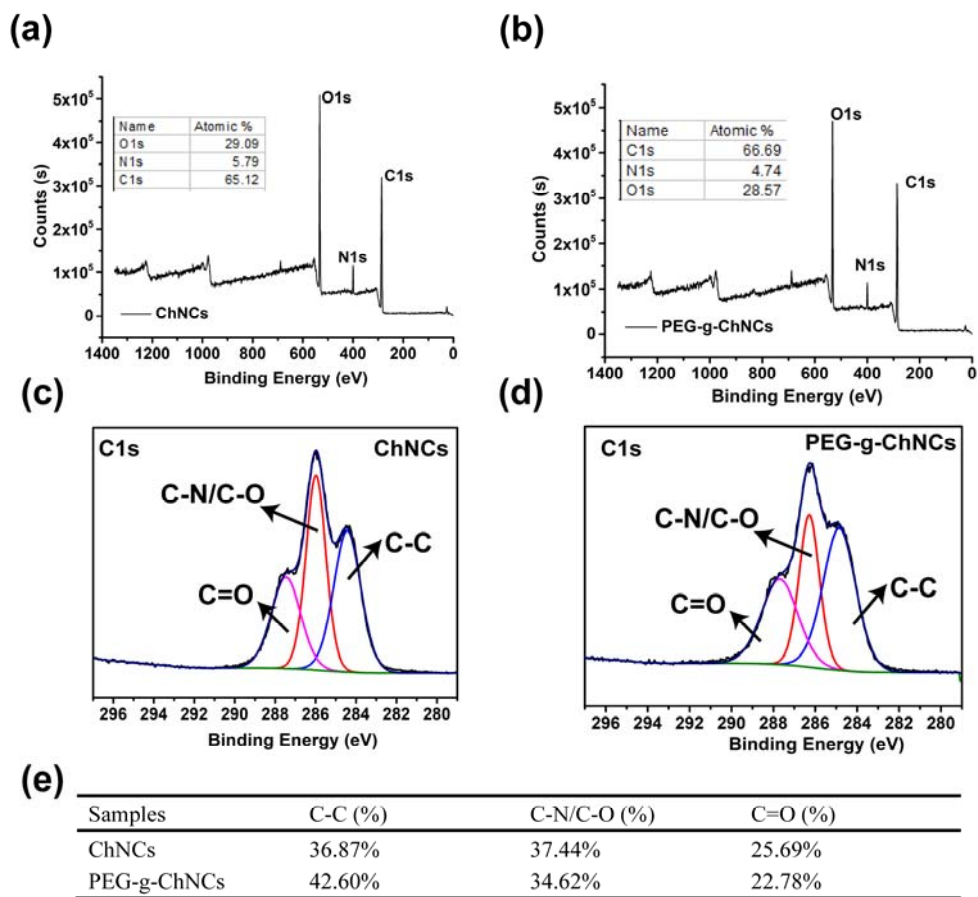


Figure S2. General XPS survey scan of ChNCs (a) and PEG-g-ChNCs (b); XPS C_{1s} spectra of ChNCs (c) and PEG-g-ChNCs (d); relative content of carbon-containing functional groups for ChNCs and PEG-g-ChNCs samples (e).

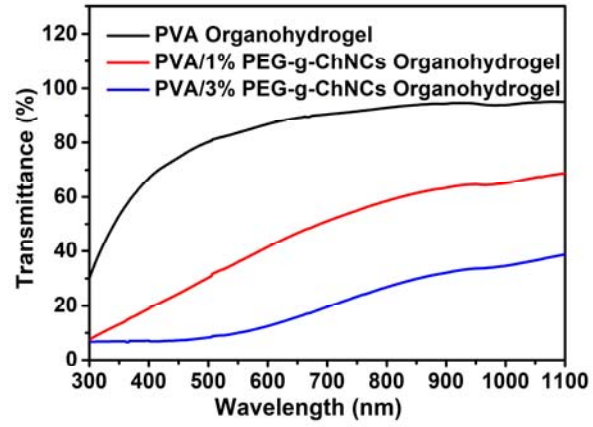


Figure S3. UV-vis transmittance of PVA/PEG-g-ChNCs organohydrogels with varying PEG-g-ChNCs contents.

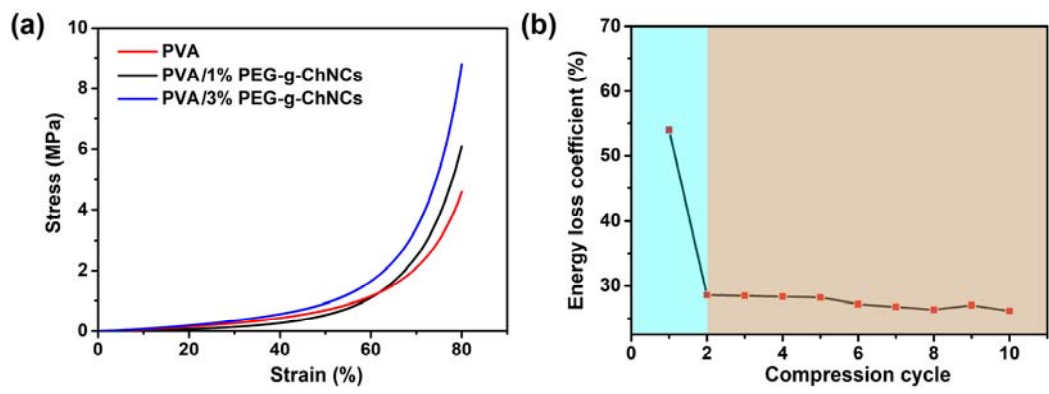


Figure S4. Compressive stress–strain curves of PVA/PEG-g-ChNCs organohydrogels with varying PEG-g-ChNCs contents (a); Energy loss coefficient of PVA/1%PEG-g-ChNCs organohydrogel vs. cyclic number for compression (b).

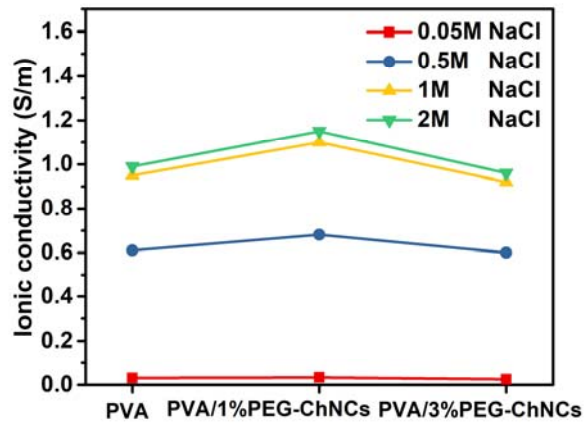


Figure S5. Ionic conductivity of PVA/1%PEG-g-ChNCs organohydrogel with varying NaCl concentrations.

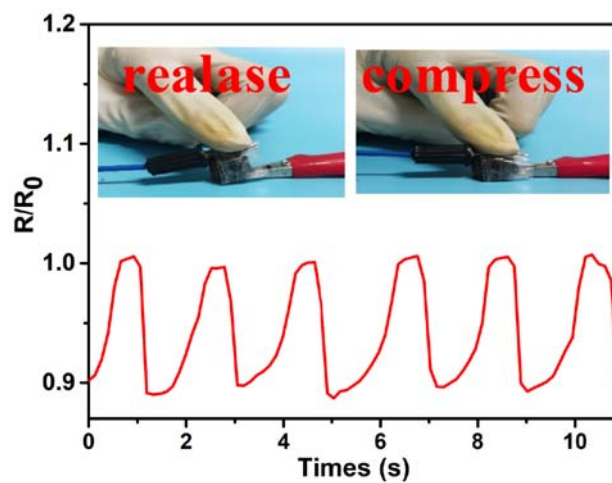


Figure S6. PVA/1%PEG-g-ChNCs organohydrogel based capacitance-type touch sensor.